

Vortex dynamics in heavy-ion-irradiated single crystals of $\text{Bi}_2\text{Sr}_2\text{CaCu}_2\text{O}_{8+\delta}$ and $\text{Bi}_{1.8}\text{Pb}_{0.2}\text{Sr}_2\text{CaCu}_2\text{O}_{8+\delta}$: Comparison from transport measurements

L. Ammor,* N. H. Hong, B. Pignon, and A. Ruyter

Laboratoire LEMA, UMR 6157 CNRS-CEA, Université F. Rabelais, UFR Sciences, Parc de Grandmont, 37200 Tours, France

(Received 6 May 2004; revised manuscript received 22 July 2004; published 7 December 2004)

Magnetotransport measurements were carried out on irradiated $\text{Bi}_2\text{Sr}_2\text{CaCu}_2\text{O}_{8+\delta}$ and $\text{Bi}_{1.8}\text{Pb}_{0.2}\text{Sr}_2\text{CaCu}_2\text{O}_{8+\delta}$ single crystals in order to investigate their vortex pinning properties. A three-dimensional Bose-glass transition with the same critical exponents is present in both cases. The occurrence of the Bose-glass transition in the case of highly anisotropic $\text{Bi}_2\text{Sr}_2\text{CaCu}_2\text{O}_{8+\delta}$ ($\gamma > 200$) supports the existence of a strong interlayer coupling of the pancake vortices due to columnar defects up to B_ϕ .

DOI: 10.1103/PhysRevB.70.224509

PACS number(s): 74.25.Fy, 74.72.Hs, 74.62.Dh

I. INTRODUCTION

Among the high-temperature superconducting cuprates (HTCS's), $\text{Bi}_2\text{Sr}_2\text{CaCu}_2\text{O}_{8+\delta}$ (BSCCO) exhibits one of the largest electromagnetic anisotropies. In such anisotropic materials, the flux lines consist of stacks of two-dimensional (2D) pancake vortices which are weakly coupled together by Josephson interactions. However, a strong anisotropy, which is caused by a highly 2D crystal structure, may cause some weak flux pinning at high temperature and under high magnetic fields. As a result, the BSCCO compound exhibits a small critical current density (J_c) and a low irreversibility line (H_{irr}). Numerous experiments, including moderate chemical doping with Pb (Refs. 1 and 2) and ion irradiation,^{3,4} have been carried out in order to improve the pinning properties in BSCCO. In these compounds, the most remarkable features are an enhancement of the critical current density J_c and an upward shift of the irreversibility line. The improved flux pinning properties in heavily Pb-doped BSCCO is supposed to stem from the lowered electronic anisotropy and the existence of strong 3D correlations in the flux line structure.^{5,6} On the other hand, heavy-ion irradiation (HII) introduces columnar defects (CD's) which may act as strong pinning centers of vortices and increase the c -axis correlation by suppressing thermal fluctuations of pancake vortices when the applied magnetic field is aligned with the defects.⁷ The observation of the uniaxial increase of pinning along the direction of the tracks in ac screening⁴ and Josephson plasma resonance⁸ measurements was considered as evidence of vortices behaving as lines rather than independent stacks of pancakes after the introduction of correlated disorder. These results are in contrast with the magnetization and torque measurements on HII BSCCO single crystals when the enhanced pinning by CD's was found to be isotropic.^{9,10} Thompson *et al.*¹⁰ reported that there is almost no difference between J_c measured under either the magnetic field applied parallel to CD's or symmetrically opposite to the c axis at an angle of 60° from the CD's. They claimed that it is due to the 2D nature of the vortex state in highly anisotropic BSCCO. Thus, the influence of the dimensionality of vortices on the vortex dynamics in heavy-ion-irradiated BSCCO with extremely large anisotropy remains unclear.

For a system of vortex lines in the presence of CD's, Nelson and Vinokur¹¹ theoretically predicted an existence of

a Bose-glass phase at temperature $T < T_{\text{BG}}$, where vortex lines are localized at the CD's. A signature of a 3D Bose-glass-to-vortex-liquid transition can be considered as the universal scaling of current-voltage characteristics with well-defined critical exponents.¹² Thus, a proof for the correlation nature of vortex pinning by CD's is the existence of the Bose-glass transition in highly anisotropic superconductor-like BSCCO.

In order to study the influence of the dimensionality of vortices on the Bose glass, we have investigated the vortex dynamics over a wide range of filling fraction and temperatures in BSCCO and $\text{Bi}_{1.8}\text{Pb}_{0.2}\text{Sr}_2\text{CaCu}_2\text{O}_{8+\delta}$ (BPSCCO) single crystals having CD's. The main difference between these two systems is their anisotropy factor γ . Our results suggested that the pancake vortices pinned by columnar tracks behave as well-coupled vortex lines at fields up to the matching field B_ϕ in irradiated BSCCO single crystals.

II. EXPERIMENT

The BSCCO (sample 1) and BPSCCO (sample 2) single crystals were-grown by a self-flux method which was described elsewhere¹³ with typical dimensions of $1 \times 1 \times 0.03 \text{ mm}^3$. Samples 1 and 2 were irradiated with 5.8-GeV Pb ions using the high-energy beam line (IRABAT facility) at Ganil (Caen, France). The electronic stopping power ($S_e \sim 32 \text{ keV/nm}$) of the Pb ions varied by less than 10% within the thickness of the samples and was sufficiently large for producing homogeneous CD's throughout the thickness of our crystals.¹⁴ Columnar tracks of diameter $2C_0 \approx 90 \text{ \AA} \pm 10 \text{ \AA}$ were created along the c axis with a matching dose of $B_\phi = 0.75 \text{ T}$ ($B_\phi = \phi_0/d$ where ϕ_0 is the elementary flux quantum and d is the mean distance between CD's). Isothermal I - V characteristics were obtained by using a dc four-probe method with a voltage resolution of 10^{-10} V and a temperature stability better than 5 mK. The contact resistance is sufficiently low to prevent heating effects up to 80 mA. More, no bulk heating effects were detected from the temperature controller. The crystal is mounted on the sample holder with its length along the rotating axis. For all samples, the zero-field Ohmic resistance as a function of the temperature did not exhibit any anomaly. An estimation of the width of the superconducting transition $\Delta T \approx 1.0$ – 1.5 K is obtained

from the width which was measured at a half maximum of the peak in $d \ln(R)/dT$. For samples 1 and 2, T_C was found to be 89.5 K and 80 K, respectively. The magnetic field was applied parallel to the CD's. A rotating sample holder is controlled by a computer with an angular resolution of about 10^{-3} deg. The angular dependence of the resistance $R(\theta)$, where θ is the angle between ab planes and the direction of the applied magnetic field, was derived from the linear part of the I - V characteristics in the vicinity of the ab planes (i.e., low angle values). Typical currents from 50 μ A to 1 mA are injected into the sample, in order to remain within the Ohmic regime.

III. RESULTS

A. Electronic anisotropy measurements

In order to determine the electronic anisotropy parameter γ for BSCCO and BPSCCO samples before irradiation, the angular dependence of the resistance was used (see Refs. 15 and 16 for details). According to the scaling approach from isotropic to anisotropic superconductors which was developed by Blatter *et al.*,¹⁷ the magnetic field H at an arbitrary angle θ with respect to the ab plane must be scaled to a reduced field as follows:

$$H\varepsilon(\theta) = H(\sin^2\theta + \cos^2\theta/\gamma^2)^{1/2}. \quad (1)$$

The angular dependence $R_{ab}(\theta)$ of BSCCO and BPSCCO single crystals measured at a given temperature close to T_C for different values of magnetic fields is shown in Fig. 1. The $\varepsilon(\theta)$ for both samples of BSCCO and BPSCCO which was extracted from the $R(\mu_0 H, \theta)$ feature is shown in Fig. 2. Referring to Eq. (1), one can see that the parameter γ can be determined from the saturated values of $\varepsilon(\theta)$ (i.e., where it becomes constant). Thus, as seen from Fig. 2, as for BSCCO, $\gamma=380$ and this value is comparable to the typical values recently found in the overdoped ($\gamma=360$ – 490), the optimally doped ($\gamma=550$), and slightly underdoped ($\gamma=800$) $\text{Bi}_2\text{Sr}_2\text{CaCu}_2\text{O}_{8+\delta}$ single crystals as well.^{18,19} In a similar way as for BPSCCO, γ was found to be 60 (see the inset of Fig. 2).

Recently, a reduction of the electromagnetic anisotropy due to a substitution of Pb for Bi in $\text{Bi}_2\text{Sr}_2\text{CaCu}_2\text{O}_{8+\delta}$ single crystals has been reported.^{20–23} Indeed, it has been shown that the Pb doping in BSCCO single crystals reduces the electromagnetic anisotropy parameter γ from 300 to 35 as the Pb content varies from 0 to 0.6 while measuring at $T=100$ K. A systematic decrease of γ with an increase of Pb-doping level was generally attributed to an enhancement of the interlayer Josephson coupling by the Pb substitution. Motohashi *et al.*²⁴ showed that after doping Pb, the penetration depth along the c axis, λ_c , which was determined from reflectivity measurements, is one order smaller than that of the optimally doped BSCCO, and it reflects a drastic enhancement of the interlayer coupling in Pb-doped BSCCO.

B. Current-voltage characteristics

The I - V curves in the vicinity of the glass-liquid transition at well-defined temperatures from a resistive state to a super-

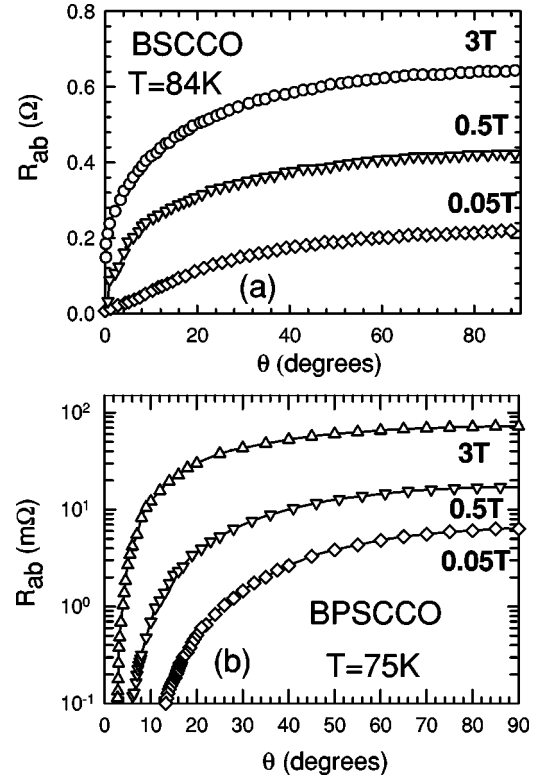


FIG. 1. $R(\theta)$ curves measured at various magnetic fields for (a) an unirradiated $\text{Bi}_2\text{Sr}_2\text{CaCu}_2\text{O}_{8+\delta}$ and (b) an unirradiated $\text{Bi}_{1.8}\text{Pb}_{0.2}\text{Sr}_2\text{CaCu}_2\text{O}_{8+\delta}$ single crystal.

conducting state ($R \equiv V/I=0$, in the low-current-density limit) were investigated (measured upon cooling, in an applied magnetic field below B_ϕ along the c axis). Note that the applied magnetic field H was aligned with the tracks by using the well-known dip feature occurring in dissipation process for $\psi_{\min} \approx 0$ (see the inset of Fig. 3) and $\psi = (\pi/2 - \theta)$ is defined as the angle between the applied field H and the crystal c axis. Typical isothermal I - V curves measured for BPSCCO (sample 2) at $f=0.333$ are shown in Fig. 3 (where

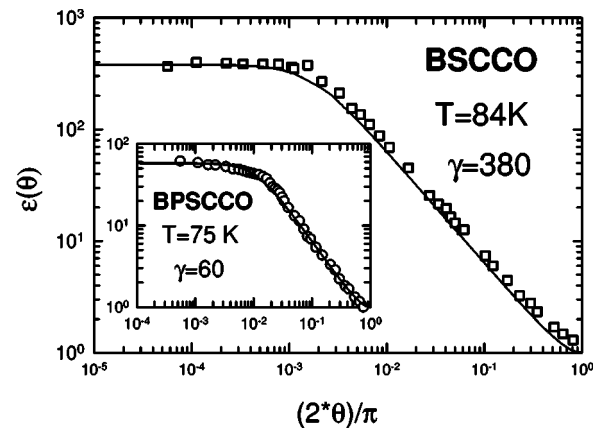


FIG. 2. Scaling parameter $\varepsilon(\theta)$ as a function of $2(\theta/\pi)$ in a log-log plot for (a) $\text{Bi}_2\text{Sr}_2\text{CaCu}_2\text{O}_{8+\delta}$ and (b) $\text{Bi}_{1.8}\text{Pb}_{0.2}\text{Sr}_2\text{CaCu}_2\text{O}_{8+\delta}$ samples. The solid lines are the classical anisotropic 3D model with an anisotropy parameter of 380 and 60 for BSCCO and BPSCCO, respectively.

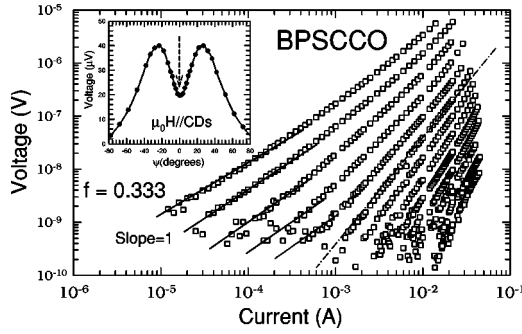


FIG. 3. Typical I - V characteristics around T_{BG} at $f=0.333$ for the irradiated $\text{Bi}_{1.8}\text{Pb}_{0.2}\text{Sr}_2\text{CaCu}_2\text{O}_{8+\delta}$ sample. From the right to the left, the data were obtained at the following temperatures: 59.38 K, 59.95 K, 60.52 K, 61.09 K, 61.67 K, 62.23 K, 62.81 K, 63.38 K, 63.96 K, 64.53 K, 65.11 K, 65.68 K, and 66.25 K. The solid lines indicate the linear response observed at high temperatures for low currents. The dashed line represents the power law dependence of $V \sim I^{(\zeta+1)/3}$ at $T=T_{BG}$, with a slope $\zeta=(z+1)/3 \sim 2$. The inset shows a typical angular dependence of the resistance, as a function of the angle ψ between the c axis and the applied magnetic field, after irradiation.

f is filling factor and $f \equiv \mu_0 H / B_\phi$. One can see that the characteristics shift from a linear response ($V \propto I$) for low current densities (solid lines) above T_{BG} to a power law regime at T_{BG} ($V \propto I^\zeta$) and finally to a strongly nonlinear response below the transition temperature ($V/I \propto \exp[-(I_0/I)^\mu]$). A very similar change in the curvature was observed in both samples. This result is expected for a glassy vortex system and basically could be explained by the Bose-glass melting theory.¹¹

According to Nelson and Vinokur,¹¹ for a Bose-glass transition in the presence of 1D correlated disorder, the melting of the Bose glass can be described by a scaling formalism in which the correlation volume diverges at $T=T_{BG}(\mu_0 H)$. This volume is anisotropic in the presence of CD's and the correlation lengths ξ_{\parallel} parallel to and ξ_{\perp} perpendicular to the columns obeying the relation $\xi_{\parallel} \propto \xi_{\perp}^\alpha$ with $\alpha=2$ in the case of screened vortex interactions ($\alpha=1$ for isotropic pinning such as point disorder as well as for an incompressible Bose-glass with long-range interactions).²⁵ The current density J which is perpendicular to the CD's and the magnetic field H aligned with the correlated defects can be derived from the following scaling ansatz:

$$\frac{E}{J_{\xi_{\parallel}}^{\xi_{\perp}^{-z}} \xi_{\perp}^{-z}} = F_{\pm} \left(\frac{J \xi_{\parallel} \xi_{\perp} \phi_0}{K_B T} \right), \quad (2)$$

where $\xi_{\perp}(T) = \xi_{\perp}(0) |(T - T_{BG}) / T_{BG}|^{-\nu_{\perp}}$, z is the critical exponent for the correlation time $\tau \propto \xi_{\perp}^z$, and F_{+} and F_{-} are two scaling functions defined in the flux liquid state ($T > T_{BG}$) and localized flux-line state ($T < T_{BG}$), respectively. The scaling function $F_{+}(x) = \text{const}$, $F_{-}(x) \propto \exp(-1/x^\mu)$ for $x \rightarrow 0$ and $F_{\pm}(x \rightarrow \infty) \propto x^{(z+1)/(1+\alpha)}$. ν_{\perp} is the critical exponent describing the divergence of the correlation lengths ξ_{\parallel} and ξ_{\perp} (note that we set $\alpha (\equiv \nu_{\parallel} / \nu_{\perp}) = 2$ in order to make the compression modulus of the vortex-liquid phase $c_{11} \sim [K_B T (\mu_0 H)^2 / \phi_0^2] / \xi_{\perp}^2 \xi_{\parallel}$ remain finite at $T=T_{BG}$ (Ref. 11)).

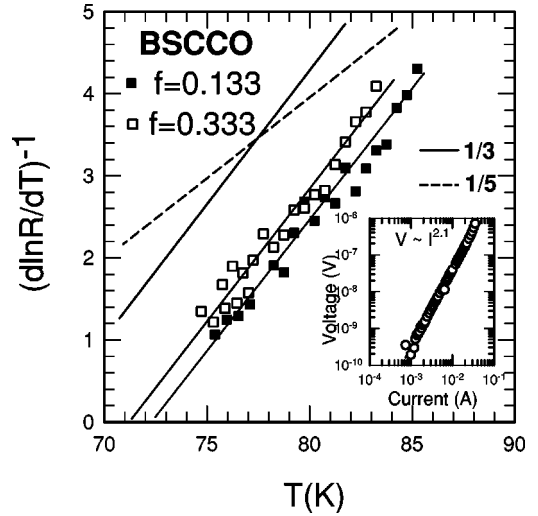


FIG. 4. Typical inverse of the logarithmic derivative of the resistance $R(T)$ for $\mu_0 H = 0.2$ T and 0.5 T. The solid lines represent the power law of $R = R_0 (T - T_{BG})^{\nu_{\perp}(z-2)}$, with a slope $[\nu_{\perp}(z-2)]^{-1} \sim 0.33$ and intercept $T_{BG} = 72.4$ K and 71 K, respectively. In comparison the dashed line represent a slope $[\nu_{\perp} z]^{-1} \sim 0.2$ which is typical for power law of $R = R_0 (T - T_{BG})^{\nu_{\perp} z}$. The inset: I - V characteristics at the solid-liquid transition. The dashed line represents the power law dependence of $V \sim I^{(\zeta+1)/3}$ at $T=T_{BG}$, with a slope $\zeta = (z+1)/3 \sim 2$.

Thus, z , ν_{\perp} , and T_{BG} are the only free parameters.

In general, from a power law dependence $V \sim I^{(\zeta+1)/3}$ at $T=T_{BG}$ and the fitting Ohmic resistance near T_{BG} in the thermally assisted flux-flow regime which should vanish according to $R \sim [(T - T_{BG}) / T_{BG}]^{\nu_{\perp}(z-2)}$, the estimated values of the dynamic exponent z and the static exponent ν_{\perp} could be determined [the slope of the solid line $\zeta = (z+1)/3$ in the inset of Fig. 4 gives $\zeta \sim 2$]. Therefore, a plot of $(d \ln R / dT)^{-1} = (T - T_{BG}) / [\nu_{\perp}(z-2)]$ versus temperature should be a straight line with a slope equal to $1 / [\nu_{\perp}(z-2)]$ intercepting the temperature axis at T_{BG} . The plot of $(d \ln R / dT)^{-1} = (T - T_{BG}) / [\nu_{\perp}(z-2)]$ versus temperature in Fig. 4 ensures this type of behavior. We obtained $[\nu_{\perp}(z-2)] \sim 3$ and $T_{BG} = 72.4$ K and 71 K, for $f=0.133$ and 0.333. Combining these two measurements, $\nu_{\perp} \sim 1$ and $z \sim 5$ were obtained.

Another special feature observed in heavy-ion-irradiated superconductors is the appearance of a minimum in the dissipation process when the vortex lines and CD's are aligned. The anisotropic pinning behavior which was predicted by the Bose-glass theory is demonstrated by the angular dependence of the voltage when the magnetic field is tilted away from the CD's direction (see Fig. 5). Figure 5(a) shows the voltage as a function of temperature under 0.3 T (i.e., $f=0.4$). Note that the field was applied at various angles $\psi = (\pi/2 - \theta)$ with respect to the CD directions for the irradiated BPSCCO single crystal. Figure 5(b) shows the evolution of this $V(\psi)$ as a function of applied magnetic field. One can see that, for the lowest T and $B < B_\phi$ values, the $V(\psi)$ curves exhibit in the vortex solid state a clear dip occurring at $\psi \sim 0$ when the field is applied along the columnar ion tracks. This pronounced downward dip of dissipation around

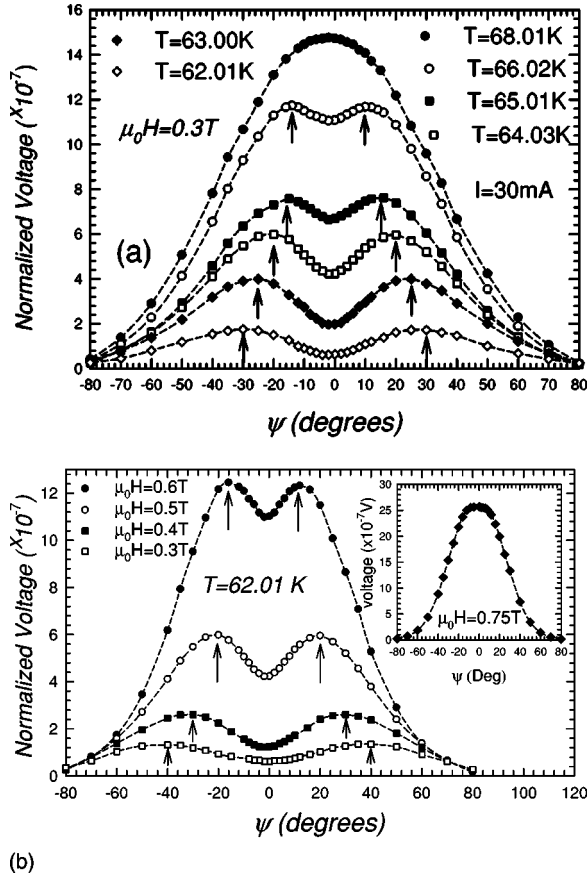


FIG. 5. Voltage as a function of the angle between the applied magnetic field and the CD's direction for irradiated BPSCCO single crystal measured in solid state with $I=30$ mA: (a) $V(\psi)$ as a function of temperature at 0.3 T. (b) $V(\psi)$ as a function of applied magnetic field at 62.01 K.

$\mu_0 H // \text{CD}'s$ is ascribed to CD pinning. When the magnetic field is tilted away from the CD's, the dissipation increases with increasing angle, indicating that the pinning by CD's remains effective up to the accommodation angle ψ_a [note that the accommodation angle ψ_a is determined experimentally as half the angular width between maximum of voltage indicated by arrows in Figs. 5(a) and 5(b)]. For BPSCCO, $\psi_a \approx 30^\circ$ at $T=62.01$ K. This increase of the voltage has been related to vortex pinning by CD's, with ψ_a as the limit of the effectiveness of CD pinning. Thus, above ψ_a , the pinning due to CD's disappears and the dissipation is more controlled by the intrinsic pinning. These results reinforce the assumption of a strong localization of the vortex at the CD's when they are aligned. Such a strong angular dependence of pinning is expected for 3D vortices, but not for extremely weak-coupling 2D pancake vortices. Similar directional properties of vortices trapped in CD's were reported by transport experiments on both moderately anisotropic layered cuprates as $\text{YBa}_2\text{Cu}_3\text{O}_{7-\delta}$ (Ref. 26) and on highly anisotropic material such as $\text{Tl}_2\text{Ba}_2\text{CaCu}_2\text{O}_8$ (Refs. 27 and 28) and were interpreted in terms of vortex-line behavior as predicted by the Bose-glass theory. In this framework the presence of CD's promotes the localization of vortices along the CD's, increasing c -axis coherence and thus leading to a directional pinning

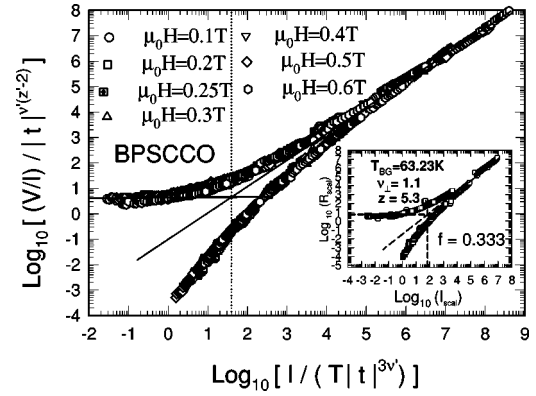


FIG. 6. Scaling forms for irradiated BPSCCO sample at indicated filling fraction of $f=0.133, 0.266, 0.333, 0.4, 0.533, 0.666,$ and 0.8 according to Eq. (2). The same scaling exponents $z=5.3 \pm 0.2$ and $\nu_\perp=1.1 \pm 0.1$ are used for all fields. The inset shows that all of the isothermal I - V curve collapse by plotting $R_{\text{scal}}=(V/I)/|t|^{\nu_\perp(z-2)}$ against $I_{\text{scal}}=I/(T|t|^{3\nu_\perp})$, using the data of Fig. 3.

enhancement. In contrast, for extremely anisotropic $\text{Bi}_2\text{Sr}_2\text{CaCu}_2\text{O}_8/\text{BiSr}_2\text{CuO}_6$ multilayers (Ref. 29) and $\text{YBa}_2\text{Cu}_3\text{O}_{7-\delta}/\text{PrBa}_2\text{Cu}_3\text{O}_{7-\delta}$ superlattices (Ref. 30) no directional effect has been shown. This result has been explained by a strongly 2D behavior of these materials.

IV. DISCUSSION

The I - V curves in the critical region scale according to Eq. (2) were separated into two curves corresponding to F_+ and F_- with the obtained exponents. From Fig. 6, it can be seen clearly that all of the I - V isothermal characteristics around T_{BG} for BPSCCO crystal at different filling factors of $f=0.133, 0.266, 0.333, 0.4, 0.533, 0.666,$ and 0.8 collapse perfectly onto two positive ($T > T_{\text{BG}}$) and negative ($T < T_{\text{BG}}$) curvature curves while plotting $R_{\text{scal}}=(V/I)/|t|^{\nu_\perp(z-2)}$ against $I_{\text{scal}}=I/(T|t|^{3\nu_\perp})$, where $t=[(T-T_{\text{BG}})/T_{\text{BG}}]$. From the scaling analysis, the optimum values of the critical exponents are $z=5.3 \pm 0.2$ and $\nu_\perp=1.1 \pm 0.1$ [i.e., $n=\nu_\perp(z-2)=3.63 \pm 0.3$]. A similar scaling behavior was obtained over a wide range of f as of 0.026, 0.04, 0.066, 0.133, 0.2, 0.266, 0.333, 0.466, 0.566, 0.666, and 0.900 for BSCCO (see the inset of Fig. 7). The vertical dashed line (for an example, see Fig. 6) gives an estimation for the current crossover separating the Ohmic and non-Ohmic behaviour J^* which can be used to evaluate the correlation length. At low temperatures, $(\xi_{\parallel}\xi_{\perp})^{1/2} \sim 20\text{--}30$ Å was obtained for both samples.

The critical exponents that we obtained are in accordance with the numerical simulations for the strongly screened vortex interactions.²⁵ Those exponents are also consistent with those reported for heavy-ion-irradiated $\text{Tl}_2\text{Ba}_2\text{CaCu}_2\text{O}_8$ thin films.³¹ In the BSCCO system, Miu *et al.*³² reported an average of the combined critical exponents $n=\nu_\perp(z-2)$ of 9 for BSCCO thin films irradiated at $B_\phi=1$ T, while Seow *et al.*⁷ obtained n as of 8.5 from the c -axis resistivity measurements on BSCCO single crystals irradiated at $B_\phi=2$ T. These two values are about 3 times larger than our results. The difference in critical exponents can be explained because columnar

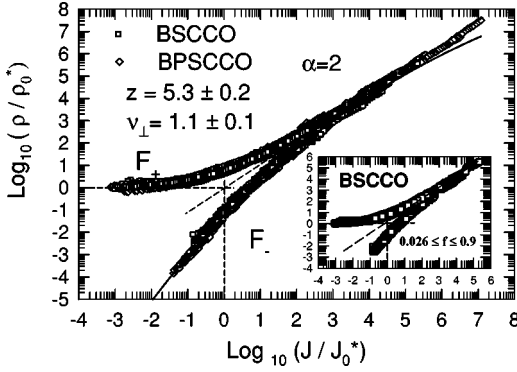


FIG. 7. Rescaled I - V characteristics using Eq. (2) obtained in both samples over a wide range of filling factors. The solid line corresponds to a variable-range hopping creep mechanism. The same scaling critical exponents are used for all fields. The inset shows scaling forms for the resistivity above and below T_{BG} at different filling factors of $f=0.026, 0.04, 0.066, 0.133, 0.266, 0.333, 0.466, 0.566, 0.666,$ and 0.900 for the BSCCO sample.

tracks are misaligned by 2° – 3° in the previous studies on irradiated BSCCO single crystals (for an example, see Ref. 7). In fact, the critical scaling behavior has been recently observed in irradiated untwinned $YBa_2Cu_3O_{7-\delta}$ single crystal only at very small angles of $-1^\circ < \psi < 1^\circ$ (Ref. 33), whereas, above 1° , there is no way to fit the data to the scaling law of the resistivity, indicating that the vortex dynamics deviates from the Bose-glass theory. Another possible explanation is that the reported exponents for irradiated BSCCO single crystals are extracted from out-of-plane transport measurements (i.e., current transport J parallel to the common direction of the magnetic field and CD's), while our critical exponents are derived from electrical transport perpendicular to the magnetic field and CD axes. For the vortex motion in the Bose glass with currents parallel to CD's and H , Nelson and Radzihovsky³⁴ predicted that above the Bose-glass transition, the longitudinal dc resistivity $\rho_{||}(T) \sim (T - T_{BG})^{\nu_{\perp} z}$ vanishes much faster than the corresponding transverse resistivity $\rho_{\perp}(T) \sim (T - T_{BG})^{\nu_{\perp}(z-2)}$. As shown in Fig. 5, in the thermally assisted flux-flow regime our data agree more with the power law $\rho_{\perp}(T) \sim (T - T_{BG})^{\nu_{\perp}(z-2)}$ than the $\rho_{||}(T) \sim (T - T_{BG})^{\nu_{\perp} z}$ power law.

The comparison with the reported n value found by Miu *et al.* on BSCCO thin films is more complicated. In fact, several possibilities have been considered to explain the difference concerning the vortex pinning by CD's between thin films and single crystals as characteristic thin-film geometry, strong influence of other defects in thin films, etc. The same discussion was reported for a large scattering in reported exponents values in either YBCO single crystals and thin films. The exponents $z \sim 2.2$ – 2.3 , $\nu_{\perp} \sim 0.9$ – 1 , and $\alpha \sim 1.1$ – 1.2 , implying an incompressible Bose glass, were obtained for YBCO crystals^{12,35} as compared to $z \sim 5.7$, $\nu_{\perp} \sim 1.8$, and $\alpha \sim 5/3$ obtained for YBCO thin films.³⁶

The data in Fig. 7, whose axes are normalized when the resistivity was measured in units of $\rho_0^*(\rho_0^* \sim \rho_n)$ and the current in units of J^* [$J^* = J_0^* |t|^{\nu_{\perp}(1+\alpha)}$ with $J_0^* = K_B T / (\xi_{0||} \xi_{0\perp})$], show that the whole set of curves obtained for both samples and various magnetic fields ($B_{\phi}/10 < \mu_0 H < B_{\phi}$) can be su-

perimposed onto two main curves. The solid line represents an attempt to fit $F^-(x) \sim \exp[-(I_0/I)^{\mu}]$ with $\mu=1/3$ which is typical for double-superkink excitations in the transport process for flux lines close to the transition. Thus, the creep process in the Bose-glass phase can be described by a variable-range hopping mechanism for both samples in the low-current limit. Two remarkable points should be emphasized here: First, z and ν_{\perp} are found for both samples to be insensitive to H over a range of fields corresponding to a filling fraction $0.133 < f < 0.9$. Second, the same scaling functions with the critical exponents $z=5.3 \pm 0.2$ and $\nu_{\perp} = 1.1 \pm 0.1$ can be used for both samples, emphasizing the universality of the transition in this field range. Moreover, it can be noted that we could not scale I - V curves for $\mu_0 H \leq B_{\phi}/10$ in either BSCCO or Pb-doped BSCCO. A very strong curvature that rapidly deviates from the high-temperature linear regime was observed and it suggests a much abrupt depinning of the vortices in this low-field range.

The experimental results obtained in both systems with very different electronic anisotropies appear to be very consistent with the Bose-glass predictions for vortex line pinned by CD's. The observed Bose-glass behavior in highly anisotropic BSCCO ($\gamma=380$) with CD's indicates that the pancake vortices pinned by columnar tracks in heavy-ion-irradiated BSCCO crystals act as well-coupled vortex lines. The 3D coupling of vortices by CD's was demonstrated by the transport measurements in flux transformer geometry³⁷ and Josephson plasma resonance in BSCCO with CD's.³⁸

Our observations are in contradiction with the interpretation of the irreversibility in terms of single-pancake depinning from CD's in Ref. 18. In fact, the directional effect (uniaxial pinning) and critical scaling up to the matching field B_{ϕ} , clearly evidenced in Pb-substituted BSCCO, are not in favor of 2D Abrikosov pancake vortices pinned by different column sites. However, the experiments in Ref. 18 were performed on an optimally doped ($\gamma=360$) or a lightly overdoped irradiated BSCCO ($\gamma=550$) and these values of γ are much higher compared to $\gamma=60$ found in our Pb-substituted BSCCO crystals. Numerous studies performed on high- T_C superconductors indicated that the value of the electronic anisotropy strongly affects the static and dynamic properties of the vortex matter in the presence of CD's.³⁹ For example, the 3D Bose glass was observed at field below the matching field B_{ϕ} by ac magnetic susceptibility measurements in irradiated BSCCO single crystals,⁴⁰ whereas the Bose-glass behavior was not observed in irradiated $Bi_2Sr_2CuO_{6+\delta}$ (Bi-2201). This difference is due to the extremely weak coupling between pancake vortices along the c axis in Bi-2201 ($\gamma=700$) even under the presence of CD's. Thus, the anisotropy is the parameter which controls the occurrence of the Bose-glass behavior in heavy-ion-irradiated BSCCO crystals.

V. CONCLUSIONS

We have presented experimental results of the I - V characteristics of heavy-ion-irradiated BPSCCO and BSCCO single crystals. The electronic anisotropy parameter was found to be $\gamma=60$ and 380 for BPSCCO and BSCCO before irradiation, respectively. The extraction of the anisotropy pa-

parameter from magnetoresistance data gives comparable values to those reported so far for BSCCO and BPSCCO. On the other hand, the vortex pinning properties in irradiated BSCCO and BPSCCO single crystals were thoroughly studied over a wide range of filling fraction and temperature. The angular measurements for both samples show that the dissipation in the vortex solid state has an usual anisotropic pinning effect when the vortex lines and the CD's are aligned. The I - V characteristics measured at $T \geq 50$ K for $B_\phi/10 < H < B_\phi$ are analyzed in terms of the critical scaling of I - V characteristics when the magnetic field is parallel to the tracks. A 3D Bose-glass transition with the same critical exponents was found in both samples. The critical exponents that we obtained, $z = 5.3 \pm 0.2$ and $\nu_\perp = 1.1 \pm 0.1$, are in accor-

dance with numerical simulations of strongly screened vortex interactions. The existence of the Bose-glass-to-liquid transition at $T_{BG}(\mu_0 H)$ in the case of highly anisotropic $\text{BiSr}_2\text{CaCu}_2\text{O}_{8+\delta}$ ($\gamma > 200$) with CD's suggests that vortices behave as lines rather than independent stacks of pancakes at fields up to the matching field B_ϕ .

ACKNOWLEDGMENTS

We gratefully acknowledge V. Hardy and F. Warmont for transport measurements on the unirradiated $\text{Bi}_2\text{Sr}_2\text{CaCu}_2\text{O}_{8+\delta}$ crystal. The authors thank Christophe Honstetter and Micheline Barbey for technical support. This work was supported by the CNRT-Région Centre (France).

*Corresponding author. FAX: + 33 02 47 36 71 21. Electronic address: ammor@delphi.phys.univ-tours.fr

- ¹K. Itaka, H. Taoka, S. Ooi, T. Shibaushi, and T. Tamegai, *Phys. Rev. B* **60**, R9951 (1999).
- ²D. Darminto, M. O. Tijia, T. Motohashi, H. Kobayashi, Y. Nakayama, J. Shimoyama, and K. Kishio, *Phys. Rev. B* **62**, 6649 (2000).
- ³D. Zech, S. L. Lee, H. Keller, G. Blatter, B. Janossy, P. H. Kes, T. W. Li, and A. A. Menovsky, *Phys. Rev. B* **52**, 6913 (1995).
- ⁴C. J. Van der Beek, M. Konczykowski, V. M. Vinokur, T. W. Li, P. H. Kes, and G. W. Crabtree, *Phys. Rev. Lett.* **74**, 1214 (1995).
- ⁵N. Musolino, S. Bals, G. van Tendeloo, N. Clayton, E. Walker, and R. Flükiger, *Physica C* **401**, 270 (2004).
- ⁶L. S. Uspenskaya, A. B. Kulakov, and A. L. Rakhmanov, *Phys. Rev. B* **68**, 104506 (2003); *Physica C* **402**, 136 (2004).
- ⁷W. S. Seow, R. A. Doyle, A. M. Cambell, G. Balakrishnan, D. McK. Paul, K. Kadowaki, and G. Wirth, *Phys. Rev. B* **53**, 14 611 (1996).
- ⁸T. Hanaguri, Y. Tsuchiya, S. Sakamoto, A. Maeda, and D. G. Steel, *Phys. Rev. Lett.* **78**, 3177 (1997).
- ⁹R. J. Drost, C. J. van der Beek, J. A. Heijn, M. Konczykowski, and P. H. Kes, *Phys. Rev. B* **58**, R615 (1998).
- ¹⁰J. R. Thompson, Y. R. Sun, H. R. Kerchner, D. K. Christen, B. C. Sales, B. C. Chakoumakos, A. D. Marwick, L. Civale, and J. O. Thomson, *Appl. Phys. Lett.* **60**, 2306 (1992).
- ¹¹D. R. Nelson and V. M. Vinokur, *Phys. Rev. B* **48**, 13 060 (1993).
- ¹²W. Jiang, N-C. Yeh, D. S. Reed, U. Kriplani, D. A. Beam, M. Konczykowski, T. A. Tombrello, and F. Holtzberg, *Phys. Rev. Lett.* **72**, 550 (1994).
- ¹³A. Ruyter, Ch. Simon, V. Hardy, M. Hervieu, and A. Maignan, *Physica C* **225**, 235 (1994).
- ¹⁴S. Hébert, V. Hardy, M. Hervieu, G. Villard, Ch. Simon, and J. Provost, *Nucl. Instrum. Methods Phys. Res. B* **146**, 545 (1998).
- ¹⁵F. Warmont, V. Hardy, J. Provost, D. Grebille, and Ch. Simon, *Phys. Rev. B* **57**, 7485 (1998).
- ¹⁶H. Raffy, S. Labdi, O. Laborde, and P. Monceau, *Phys. Rev. Lett.* **66**, 2515 (1991).
- ¹⁷G. Blatter, V. B. Geshkenbein, and A. I. Larkin, *Phys. Rev. Lett.* **68**, 875 (1992).
- ¹⁸C. J. Van der Beek, M. Konczykowski, A. V. Samoilov, N. Chikumoto, S. Bouffard, and M. V. Feigel'man, *Phys. Rev. Lett.* **86**,

5136 (2001).

- ¹⁹M. Tokunaga, M. Kobayashi, Y. Tokunaga, and T. Tamegai, *Phys. Rev. B* **66**, 060507(R) (2002).
- ²⁰T. Motohashi, Y. Nakayama, T. Fujita, K. Kitazawa, J. Shimoyama, and K. Kishio, *Phys. Rev. B* **59**, 14 080 (1999).
- ²¹I. Chong, Z. Hiroi, M. Izumi, J. Shimoyama, Y. Nakayama, K. Kishio, T. Terashima, Y. Bando, and M. Takano, *Science* **276**, 770 (1997).
- ²²N. Musolino, S. Bals, G. van Tendeloo, N. Clayton, E. Walker, and R. Flükiger, *Physica C* **399**, 1 (2003).
- ²³M. Bazilijevich, D. Giller, M. McElfresh, Y. Abulafia, Y. Radzyner, J. Schneck, T. H. Johansen, and Y. Yeshurun, *Phys. Rev. B* **62**, 4058 (2000).
- ²⁴T. Motohashi, J. Shimoyama, K. Kitazawa, and K. Kishio, *Phys. Rev. B* **61**, R9269 (2000).
- ²⁵A. Vestergren, J. Lidmar, and M. Wallin, *Phys. Rev. B* **67**, 092501 (2003); J. Lidmar and M. Wallin, *Europhys. Lett.* **47**, 494 (1999); M. Wallin, E. S. Sorensen, S. M. Girvin, and A. P. Young, *Phys. Rev. B* **49**, 12 115 (1994).
- ²⁶W. K. Kwok, L. M. Paulius, V. M. Vinokur, A. M. Petrean, R. M. Ronningen, and G. W. Crabtree, *Phys. Rev. B* **58**, 14 594 (1998).
- ²⁷R. C. Budhani, W. L. Holstein, and M. Suenaga, *Phys. Rev. Lett.* **72**, 566 (1994).
- ²⁸K. E. Gray, J. D. Hettinger, D. J. Miller, B. R. Washburn, C. Moreau, and C. Lee, *Phys. Rev. B* **54**, 3622 (1996).
- ²⁹A. Pomar, L. Martel, Z. Z. Li, O. Laborde, and H. Raffy, *Phys. Rev. B* **63** 020504(R) (2001).
- ³⁰B. Holzapfel, G. Kreiselmeyer, S. Bouffard, S. Klaumuzer, and L. Schultz, *Phys. Rev. B* **48**, 600 (1993).
- ³¹V. Ta Phuoc, A. Ruyter, L. Ammor, A. Wahl, and J. C. Soret, *Phys. Rev. B* **56**, 122 (1997).
- ³²L. Miu, P. Wagner, A. Hadish, F. Hilmer, and H. Adrian, *Phys. Rev. B* **51**, 3953 (1995).
- ³³R. J. Olsson, W-K. Kwok, L. M. Paulius, A. M. Petrean, D. J. Hofman, and G. W. Crabtree, *Phys. Rev. B* **65**, 104520 (2002).
- ³⁴D. R. Nelson and L. Radzihovsky, *Phys. Rev. B* **54**, R6845 (1996).
- ³⁵D. S. Reed, N. C. Yeh, M. Konczykowski, A. V. Samoilov, and F. Holtzberg, *Phys. Rev. B* **51**, 16 448 (1995).
- ³⁶G. Nakielski, A. Rickertsen, T. Steiborn, J. Wiesner, G. Wirth, A.

- G. M. Jansen, and J. Kötzler, Phys. Rev. Lett. **76**, 2567 (1996).
- ³⁷R. A. Doyle, W. S. Seow, Y. Yan, A. M. Cambell, T. Mochiku, K. Kadowaki, and G. Wirth, Phys. Rev. Lett. **77**, 1155 (1996).
- ³⁸T. Hanaguri, Y. Tsuchiya, S. Sakamoto, A. Maeda, and D. G. Steel, Phys. Rev. Lett. **78**, 3177 (1997).
- ³⁹V. Hardy, A. Wahl, S. Hebert, A. Ruyter, J. Provot, D. Groult, and Ch. Simon, Phys. Rev. B **54**, 656 (1996).
- ⁴⁰N. Kuroda, N. Ishikawa, Y. Chimi, A. Iwase, R. Yoshzaki, and T. Kambara, Physica C **321**, 143 (1999).